DESY 16-090
May 2016

Multiquark Hadrons - A New Facet of QCD*

Ahmed Ali *

Deutsches Elektronen-Synchrotron DESY,
D-22607 Hamburg, Germany
* *E-mail: ahmed.ali@desy.de*

I review some selected aspects of the phenomenology of multiquark states discovered in high energy experiments. They have four valence quarks (called tetraquarks) and two of them are found to have five valence quarks (called pentaquarks), extending the conventional hadron spectrum which consists of quark-antiquark ($q\bar{q}$) mesons and qqq baryons. Multiquark states represent a new facet of QCD and their dynamics is both challenging and currently poorly understood. I discuss various approaches put forward to accommodate them, with emphasis on the diquark model.

Keywords: Exotic Hadrons, Tetraquarks, Pentaquarks, Hadron Molecules

1. Introduction

Ever since the discovery of the state $X(3870)$ by Belle in 2003[1], a large number of multiquark states has been discovered in particle physics experiments (see recent reviews[2–6]). Most of them are quarkonium-like states, in that they have a $(c\bar{c})$ or a $(b\bar{b})$ component in their Fock space. A good fraction of them is electrically neutral but some are singly-charged. Examples are $X(3872)(J^{PC} = 1^{++})$, $Y(4260)(J^{PC} = 1^{--})$, $Z(3900)^{\pm}(J^P = 1^+)$, $P_c(4450)^{\pm}(J^P = 5/2^+)$, in the hidden charm sector, and $Y_b(10890)(J^{PC} = 1^{--})$, $Z_b(10610)^{\pm}(J^P = 1^+)$ and $Z_b(10650)^{\pm}(J^P = 1^+)$, in the hidden bottom sector. The numbers in the parentheses are their masses in MeV. Of these, $P_c(4450)^{\pm}(J^P = 5/2^+)$ is a pentaquark state, as its discovery mode $P_c(4450)^+ \to J/\psi p$ requires a minimal valence quark content $c\bar{c}uud$. The others are tetraquark states, with characteristic decays, such as $X(3872) \to J/\psi\pi^+\pi^-$, $Y(4260) \to J/\psi\pi^+\pi^-$, $Z(3900)^+ \to J/\psi\pi^+$, $Y_b(10890) \to \Upsilon(1S, 2S, 3S)\pi^+\pi^-$, and $Z_b(10610)^+ \to h_b(1P, 2P)\pi^{\pm}, \Upsilon(1S, 2S)\pi^+$. No

*To be published in the proceedings of the 14th. Regional Conference on Mathematical Physics, Quaid-i-Azam University, Islamabad, Nov. 9-14, 2015.

doubly-charged multiquark hadron has been seen so far, though some are expected, such as $[\bar{c}\bar{u}][sd] \to D_s^- \pi^-$, in the tetraquark scenario discussed below.

Deciphering the underlying dynamics of the multiquark states is a formidable challenge and several models have been proposed to accommodate them. They include, among others, cusps[7,8], which assume that the final state rescatterings are enough to describe data, and as such there is no need for poles in the scattering matrix. This is the minimalist approach, in particular, invoked to explain the origin of the charged states $Z_c(3900)$ and $Z(4025)$. If proven correct, one would have to admit that all this excitement about new frontiers of QCD is "much ado about nothing".

A good majority of the interested hadron physics community obviously does not share this agnostic point of view, and dynamical mechanisms have been devised to accommodate the new spectroscopy. One such model put forward to accommodate the exotic hadrons is hadroquarkonium, in which a $Q\bar{Q}$ ($Q = c, b$) forms the hard core surrounded by light matter (light $q\bar{q}$ states). For example, the hadrocharmonium core may consist of $J/\psi, \psi', \chi_c$ states, and the light $q\bar{q}$ degrees of freedom can be combined to accommodate the observed hadrons[9]. This is motivated by analogy with the good old hydrogen atom which explained a lot of atomic physics. A variation on this theme is that the hard core quarkonium could be in a color-adjoint representation, in which case the light degrees of freedom are also a color-octet to form an overall singlet.

Next are hybrid models, the basic idea of which dates back to circa 1994[10] based on the QCD-inspired flux-tubes, which predict exotic $J^{\rm PC}$ states of both the light and heavy quarks. Hybrids are hadrons formed from the valence quarks and gluons, for example, consisting of $q\bar{q}g$. In the context of the X, Y, Z hadrons, hybrids have been advanced as a model for the $J^{\rm PC} = 1^{--}$ state $Y(4260)$, which has a small e^+e^- annihilation cross section[11–13], But, hybrids have been offered as templates for other exotic hadrons as well[14,15].

Another popular approach assumes that the multiquark states are meson-meson and meson-baryon bound states, with an attractive residual van der Waals force generated by mesonic exchanges[16]. This hypothesis is in part supported by the closeness of the observed exotic hadron masses to the respective meson-meson (meson-baryon) thresholds. In many cases, this leads to very small binding energy, which imparts them a very large hadronic radius. This is best illustrated by $X(3872)$, which has an S-wave coupling to $D^*\bar{D}$ (and its conjugate) and has a binding en-

ergy $\mathcal{E}_X = M_{X(3872)} - M_{D^{*0}} - M_{\bar{D}^0} = -0.3 \pm 0.4$ MeV. Such a hadron molecule will have a large mean square separation of the constituents $\langle r_X \rangle \propto 1/\sqrt{\mathcal{E}_X} \simeq 5$ fm, where the quoted radius corresponds to a binding energy $\mathcal{E}_X = 0.3$ MeV. This would lead to small production cross-sections in hadronic collisions[17], contrary to what has been observed in a number of experiments at the Tevatron and the LHC. In some theoretical constructs, this problem is mitigated by making the hadron molecules complicated by invoking a hard (point-like) core. In that sense, such models resemble hadroquarkonium models, discussed above. In yet others, rescattering effects are invoked to substantially increase the cross-sections[18]. Theoretical interest in hadron molecules has remained unabated, and there exists a vast and growing literature on this topic with ever increasing sophistication, a sampling of which is referenced here [19–25].

Last, but by no means least, on this list are QCD-based interpretations in which tetraquarks and pentaquarks are genuinely new hadron species[26–28]. In the large N_c limit of QCD, tetraquarks are shown to exist[29–31] as poles in the S-matrix, and they may have narrow widths in this approximation, and hence they are reasonable candidates for multiquark states. First attempts using Lattice QCD have been undertaken[32,33] in which correlations involving four-quark operators are studied numerically. Evidence of tetraquark states in the sense of S-matrix poles using these methods is still lacking. Establishing the signal of a resonance requires good control of the background. In the lattice QCD simulations of multiquark states, this is currently not the case. This may be traced back to the presence of a number of nearby hadronic thresholds and to lattice-specific issues, such as an unrealistic pion mass. More powerful analytic and computational techniques are needed to draw firm conclusions. In the absence of reliable first principle calculations, approximate phenomenological methods are the only way forward. In that spirit, an effective Hamiltonian approach has been often used[26,27,34–37], in which tetraquarks are assumed to be diquark-antidiquark objects, bound by gluonic exchanges (pentaquarks are diquark-diquark-antiquark objects). This allows one to work out the spectroscopy and some aspects of tetraquark decays. Heavy quark symmetry is a help in that it can be used for the heavy-light diquarks relating the charmonia-like states to the bottomonium-like counterparts. I will be mainly discussing interpretations of the current data based on the phenomenological diquark picture to test how far such models go in describing the observed exotic hadrons and other properties measured in current experiments.

2. The Diquark Model

The basic assumption of this model is that diquarks are tightly bound colored objects and they are the building blocks for forming tetraquark mesons and pentaquark baryons. The diquarks, for which we use the notation $[qq]_c$, and interchangeably $\mathcal{Q}$, have two possible SU(3)-color representations. Since quarks transform as a triplet $\mathsf{3}$ of color SU(3), the diquarks resulting from the direct product $\mathsf{3} \otimes \mathsf{3} = \bar{\mathsf{3}} \oplus \mathsf{6}$, are thus either a color anti-triplet $\bar{\mathsf{3}}$ or a color sextet $\mathsf{6}$. The leading diagram based on one-gluon exchange is shown below.

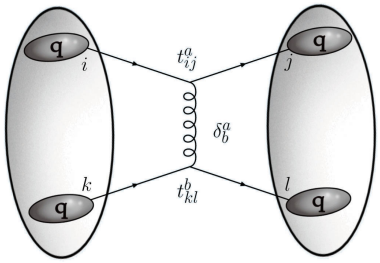

Fig. 1. One-gluon exchange diagram for diquarks.

The product of the SU(3)-matrices in Fig. 1 can be decomposed as

$$t^a_{ij}t^a_{kl} = -\frac{2}{3}\underbrace{(\delta_{ij}\delta_{kl} - \delta_{il}\delta_{kj})/2}_{\text{antisymmetric: projects } \bar{\mathbf{3}}} + \frac{1}{3}\underbrace{(\delta_{ij}\delta_{kl} + \delta_{il}\delta_{kj})/2}_{\text{symmetric: projects } \mathbf{6}} .$$

The coefficient of the antisymmetric $\bar{\mathsf{3}}$ representation is $-2/3$, reflecting that the two diquarks bind with a strength half as strong as between a quark and an antiquark, in which case the corresponding coefficient is $-4/3$. The symmetric $\mathsf{6}$ on the other hand has a positive coefficient, $+1/3$, reflecting a repulsion. This perturbative argument is in agreement with lattice QCD simulations[38]. Thus, in working out the phenomenology, a diquark is assumed to be an $SU(3)_c$-antitriplet, with the antidiquark a color-triplet. With this, we have two color-triplet fields, quark q_3 and anti-diquark $\overline{\mathcal{Q}}$ or $[\bar{q}\bar{q}]_3$, and two color-antitriplet fields, antiquark $\bar{q}_{\bar{3}}$ and diquark $\mathcal{Q}$ or $[qq]_{\bar{3}}$, from which the spectroscopy of the conventional and exotic hadrons is built.

Since quarks are spin-1/2 objects, a diquark has two possible spin-configurations, spin-0, with the two quarks in a diquark having their spin-vectors anti-parallel, and spin-1, in which case the two quark spins are

aligned, as shown in Fig. 2. They were given the names "good diquarks"

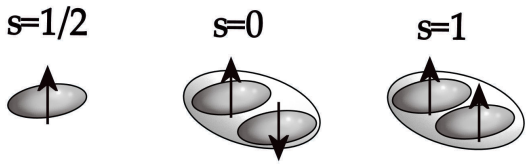

Fig. 2. Quark and diquark spins.

and "bad diquarks", respectively, by Jaffe[39], implying that in the former case, the two quarks bind, and in the latter, the binding is not as strong. There is some support of this pattern from lattice simulations for light diquarks[38]. However, as the spin-degree of freedom decouples in the heavy quark systems, as can be shown explicitly in heavy quark effective theory context for heavy mesons and baryons, we expect that this decoupling will also hold for heavy-light diquarks $[Q_i q_j]_{\bar{3}}$ with $Q_i = c, b; q_j = u, d, s$. So, for the heavy-light diquarks, both the spin-1 and spin-0 configurations are present. Also, what concerns the diquarks in heavy baryons (such as Λ_b and Ω_b), consisting of a heavy quark and a light diquark, both $j^p = 0^+$ and $j^p = 1^+$ quantum numbers of the diquark are needed to accommodate the observed baryon spectrum.

In this lecture, we will be mostly discussing heavy-light diquarks, and following the discussion above, we construct the interpolating diquark operators for the two spin-states of such diquarks (here $Q = c, b$)[27]:

$$\begin{array}{rlcl} \text{Scalar} & 0^+: & \mathcal{Q}_{i\alpha} & = \epsilon_{\alpha\beta\gamma}(\bar{Q}_c^{\beta}\gamma_5 q_i^{\gamma} - \bar{q}_{i_c}^{\beta}\gamma_5 Q^{\gamma}), \\ \text{Axial-Vector} & 1^+: & \vec{\mathcal{Q}}_{i\alpha} & = \epsilon_{\alpha\beta\gamma}(\bar{Q}_c^{\beta}\vec{\gamma} q_i^{\gamma} + \bar{q}_{i_c}^{\beta}\vec{\gamma} Q^{\gamma}). \end{array} \qquad \alpha, \beta, \gamma\text{: } SU(3)_C \text{ indices}$$

In the non-relativistic (NR) limit, these states are parametrized by Pauli matrices: $\Gamma^0 = \frac{\sigma_2}{\sqrt{2}}$(Scalar 0^+), and $\vec{\Gamma} = \frac{\sigma_2\vec{\sigma}}{\sqrt{2}}$(Axial-Vector 1^+). We will characterize a tetraquark state with total angular momentum J by the state vector $\left|Y_{[bq]}\right\rangle = |s_{\mathcal{Q}}, s_{\bar{\mathcal{Q}}};\ J\rangle$ showing the diquark spin $s_{\mathcal{Q}}$ and the antidiquark spin $s_{\bar{\mathcal{Q}}}$. Thus, the tetraquarks with the following diquark-spin

and angular momentum J have the Pauli forms:

$$
\begin{aligned}
|0_{\mathcal{Q}}, 0_{\bar{\mathcal{Q}}};\ 0_J\rangle &= \Gamma^0 \otimes \Gamma^0, \\
|1_{\mathcal{Q}}, 1_{\bar{\mathcal{Q}}};\ 0_J\rangle &= \frac{1}{\sqrt{3}}\Gamma^i \otimes \Gamma_i \ldots, \\
|0_{\mathcal{Q}}, 1_{\bar{\mathcal{Q}}};\ 1_J\rangle &= \Gamma^0 \otimes \Gamma^i, \\
|1_{\mathcal{Q}}, 0_{\bar{\mathcal{Q}}};\ 1_J\rangle &= \Gamma^i \otimes \Gamma^0, \\
|1_{\mathcal{Q}}, 1_{\bar{\mathcal{Q}}};\ 1_J\rangle &= \frac{1}{\sqrt{2}}\varepsilon^{ijk}\Gamma_j \otimes \Gamma_k.
\end{aligned}
$$

2.1. *NR Hamiltonian for Tetraquarks with hidden charm*

For the heavy quarkonium-like exotic hadrons, we work in the non-relativistic limit and use the following effective Hamiltonian to calculate the tetraquark mass spectrum [27,34]

$$H_{\rm eff} = 2m_{\mathcal{Q}} + H_{SS}^{(qq)} + H_{SS}^{(q\bar{q})} + H_{SL} + H_{LL},$$

where $m_{\mathcal{Q}}$ is the diquark mass, the second term above is the spin-spin interaction involving the quarks (or antiquarks) in a diquark (or anti-diquark), the third term depicts spin-spin interactions involving a quark and an antiquark in two different shells, with the fourth and fifth terms being the spin-orbit and the orbit-orbit interactions, involving the quantum numbers of the tetraquark, respectively. For the S-states, these last two terms are absent. For illustration, we consider the case $Q = c$ and display the individual terms in $H_{\rm eff}$:

$$
\begin{aligned}
H_{SS}^{(qq)} &= 2(\mathcal{K}_{cq})_{\bar{3}}[(\mathbf{S}_c \cdot \mathbf{S}_q) + (\mathbf{S}_{\bar{c}} \cdot \mathbf{S}_{\bar{q}})], \\
H_{SS}^{(q\bar{q})} &= 2(\mathcal{K}_{c\bar{q}})(\mathbf{S}_c \cdot \mathbf{S}_{\bar{q}} + \mathbf{S}_{\bar{c}} \cdot \mathbf{S}_q) + 2\mathcal{K}_{c\bar{c}}(\mathbf{S}_c \cdot \mathbf{S}_{\bar{c}}) + 2\mathcal{K}_{q\bar{q}}(\mathbf{S}_q \cdot \mathbf{S}_{\bar{q}}), \\
H_{SL} &= 2A_{\mathcal{Q}}(\mathbf{S}_{\mathcal{Q}} \cdot \mathbf{L} + \mathbf{S}_{\bar{\mathcal{Q}}} \cdot \mathbf{L}), \\
H_{LL} &= B_{\mathcal{Q}} \tfrac{L_{\mathcal{Q}\bar{\mathcal{Q}}}(L_{\mathcal{Q}\bar{\mathcal{Q}}}+1)}{2}.
\end{aligned}
$$

The usual angular momentum algebra then yields the following form:

$$
\begin{aligned}
H_{\rm eff} &= 2m_{\mathcal{Q}} + \frac{B_{\mathcal{Q}}}{2}\langle \boldsymbol{L}^2\rangle - 2a\langle \boldsymbol{L}\cdot\boldsymbol{S}\rangle + 2\kappa_{qc}\big[\langle \boldsymbol{s_q}\cdot\boldsymbol{s_c}\rangle + \langle \boldsymbol{s_{\bar{q}}}\cdot\boldsymbol{s_{\bar{c}}}\rangle\big] \\
&= 2m_{\mathcal{Q}} - aJ(J+1) + \left(\frac{B_{\mathcal{Q}}}{2} + a\right)L(L+1) + aS(S+1) - 3\kappa_{qc} \\
&\quad + \kappa_{qc}\big[s_{qc}(s_{qc}+1) + s_{\bar{q}\bar{c}}(s_{\bar{q}\bar{c}}+1)\big].
\end{aligned}
$$

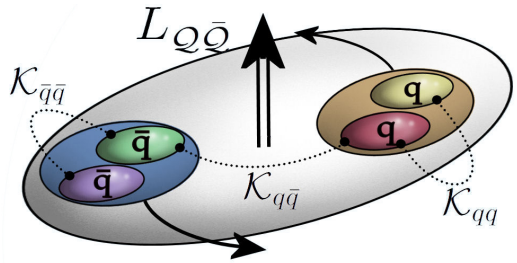

Fig. 3. Schematic diagram of a tetraquark in the diquark-antidiquark picture.

2.2. *Low-lying S and P-wave tetraquark states in the $c\bar{c}$ and $b\bar{b}$ sectors*

The states in the diquark-antidiquark basis $|s_{qQ}, s_{\bar{q}\bar{Q}}; S, L\rangle_J$ and in the $Q\bar{Q}$ and $q\bar{q}$ basis $|s_{q\bar{q}}, s_{Q\bar{Q}}; S', L'\rangle_J$ are related by Fierz transformation. The positive parity S-wave tetraquarks are given in terms of the six states listed in Table 1 (charge conjugation is defined for neutral states). These states are characterized by the quantum number $L = 0$, hence their masses depend on just two parameters M_{00} and κ_{qQ}, leading to several predictions to be tested against experiments. The P-wave states are listed in Table 2. The first four of them have $L = 1$, and the fifth has $L = 3$, and hence is expected to be significantly heavier.

Table 1. S-wave tetraquark states in two bases and their masses in the diquark model.

Label	J^{PC}	$\|s_{qQ}, s_{\bar{q}\bar{Q}}; S, L\rangle_J$	$\|s_{q\bar{q}}, s_{Q\bar{Q}}; S', L'\rangle_J$	Mass
X_0	0^{++}	$\|0,0;0,0\rangle_0$	$\big(\|0,0;0,0\rangle_0 + \sqrt{3}\|1,1;0,0\rangle_0\big)/2$	$M_{00} - 3\kappa_{qQ}$
X_0'	0^{++}	$\|1,1;0,0\rangle_0$	$\big(\sqrt{3}\|0,0;0,0\rangle_0 - \|1,1;0,0\rangle_0\big)/2$	$M_{00} + \kappa_{qQ}$
X_1	1^{++}	$\big(\|1,0;1,0\rangle_1 + \|0,1;1,0\rangle_1\big)/\sqrt{2}$	$\|1,1;1,L'\rangle_1$	$M_{00} - \kappa_{qQ}$
Z	1^{+-}	$\big(\|1,0;1,0\rangle_1 - \|0,1;1,0\rangle_1\big)/\sqrt{2}$	$\big(\|1,0;1,L'\rangle_1 - \|0,1;1,L'\rangle_1\big)/\sqrt{2}$	$M_{00} - \kappa_{qQ}$
Z'	1^{+-}	$\|1,1;1,0\rangle_1$	$\big(\|1,0;1,L'\rangle_1 + \|0,1;1,L'\rangle_1\big)/\sqrt{2}$	$M_{00} + \kappa_{qQ}$
X_2	2^{++}	$\|1,1;2,0\rangle_2$	$\|1,1;2,L'\rangle_2$	$M_{00} + \kappa_{qQ}$

The parameters appearing on the r.h. columns of Tables 1 and 2 can be determined using the masses of some of the observed X, Y, Z states, and their numerical values are given in Table 3. Some parameters in the $c\bar{c}$ and $b\bar{b}$ sectors can also be related using the heavy quark mass scaling [40].

Typical errors on the masses due to parametric uncertainties are estimated to be about 30 MeV. As we see from table 4, there are lot more X, Y, Z hadrons observed in experiments in the charmonium-like sector than

Table 2. P-wave tetraquark states in two bases and their masses in the diquark model.

Label	J^{PC}	$\|s_{qQ}, s_{\bar{q}\bar{Q}}; S, L\rangle_J$	$\|s_{q\bar{q}}, s_{Q\bar{Q}}; S', L'\rangle_J$	Mass
Y_1	1^{--}	$\|0,0;0,1\rangle_1$	$\big(\|0,0;0,1\rangle_1 + \sqrt{3}\|1,1;0,1\rangle_1\big)/2$	$M_{00} - 3\kappa_{qQ} + B_Q$
Y_2	1^{--}	$\big(\|1,0;1,1\rangle_1 + \|0,1;1,1\rangle_1\big)/\sqrt{2}$	$\|1,1;1,L'\rangle_1$	$M_{00} - \kappa_{qQ} + 2a + B_Q$
Y_3	1^{--}	$\|1,1;0,1\rangle_1$	$\big(\sqrt{3}\|0,0;0,1\rangle_1 - \|1,1;0,1\rangle_1\big)/2$	$M_{00} + \kappa_{qQ} + B_Q$
Y_4	1^{--}	$\|1,1;2,1\rangle_1$	$\|1,1;2,L'\rangle_1$	$M_{00} + \kappa_{qQ} + 6a + B_Q$
Y_5	1^{--}	$\|1,1;2,3\rangle_1$	$\|1,1;2,L'\rangle_1$	$M_{00} + \kappa_{qQ} + 16a + 6B_Q$

Table 3. Numerical values of the parameters in $H_{\rm eff}$.

	charmonium-like	bottomonium-like
M_{00} [MeV]	3957	10630
κ_{qQ} [MeV]	67	23
B_Q [MeV]	268	329
a [MeV]	52.5	26

Table 4. X, Y, Z hadron masses from experiments and in the diquark-model.

		charmonium-like		bottomonium-like	
Label	J^{PC}	State	Mass [MeV]	State	Mass [MeV]
X_0	0^{++}	—	3756	—	10562
X_0'	0^{++}	—	4024	—	10652
X_1	1^{++}	$X(3872)$	3890	—	10607
Z	1^{+-}	$Z_c^+(3900)$	3890	$Z_b^{+,0}(10610)$	10607
Z'	1^{+-}	$Z_c^+(4020)$	4024	$Z_b^+(10650)$	10652
X_2	2^{++}	—	4024	—	10652
Y_1	1^{--}	$Y(4008)$	4024	$Y_b(10891)$	10891
Y_2	1^{--}	$Y(4260)$	4263	$Y_b(10987)$	**10987**
Y_3	1^{--}	$Y(4290)$ (or $Y(4220)$)	4292	—	**10981**
Y_4	1^{--}	$Y(4630)$	4607	—	11135
Y_5	1^{--}	—	6472	—	13036

in the bottomonium-like sector, with essentially three entries $Z_b^+(10610)$, $Z_b^+(10650)$ and $Y_b(10891)$ in the latter case. There are several predictions in the charmonium-like sector, which, with the values of the parameters given in the tables above, are in the right ball-park [a]. It should be remarked that these input values, in particular for the quark-quark couplings

[a] I thank Satoshi Mishima for providing these estimates.

in a diquark, κ_{qQ}, are larger than in the earlier determinations of the same by Maiani *et al.*[27]. Better agreement is reached with experiments assuming that diquarks are more tightly bound than suggested from the analysis of the baryons in the diquark-quark picture, and the spectrum shown here is in agreement with the one in the modified scheme[34]. Alternative calculations of the tetraquark spectrum based on diquark-antidiquark model have been carried out[41].

The exotic bottomonium-like states are currently rather sparse. The reason for this is that quite a few exotic charmonium-like states were observed in the decays of B-hadrons. This mode is obviously not available for the hidden $b\bar{b}$ states. They can only be produced in hadro- and electroweak high energy processes. Tetraquark states with a single b quark can, in principle, also be produced in the decays of the B_c mesons, as pointed out recently[42]. As the $c\bar{c}$ and $b\bar{b}$ cross-section at the LHC are very large, we anticipate that the exotic spectroscopy involving the open and hidden heavy quarks is an area where significant new results will be reported by all the LHC experiments. Measurements of the production and decays of exotica, such as transverse-momentum distributions and polarization information, will go a long way in understanding the underlying dynamics.

As a side remark, we mention that recently there has been a lot of excitement due to the D0 observation[43] of a narrow structure $X(5568)$, consisting of four different quark flavors ($bdus$), found through the $B_s^0\pi^\pm$ decay mode. However, this has not been confirmed by the LHCb collaboration[44], despite the fact that LHCb has 20 times higher B_s^0 sample than that of D0. This would have been the first discovery of an open b-quark tetraquark state. They are anticipated in the compact tetraquark picture[42], and also in the hadron molecule framework[45]. We wait for more data from the LHC experiments.

We now discuss the three observed exotic states in the bottomonium sector in detail. The hidden $b\bar{b}$ state $Y_b(10890)$ with $J^{\rm P} = 1^{--}$ was discovered by Belle in 2007[46] in the process $e^+e^- \to Y_b(10890) \to (\Upsilon(1S), \Upsilon(2S), \Upsilon(3S))\pi^+\pi^-$ just above the $\Upsilon(5S)$. The branching ratios measured are about two orders of magnitude larger than anticipated from similar dipionic transitions in the lower $\Upsilon(nS)$ states and ψ' (for a review and references to earlier work, see Brambilla *et al*[47].). Also the dipion invariant mass distributions in the decays of Y_b are marked by the presence of the resonances $f_0(980)$ and $f_2(1270)$. This state was interpreted as a $J^{\rm PC} = 1^{--}$ P-wave tetraquark[35,36]. Subsequent to this, a Van Royen-Weiskopf formalism was used[37] in which direct electromagnetic couplings

with the diquark-antidiquark pair of the Y_b was assumed. Due to the P-wave nature of the $Y_b(10890)$, with a commensurate small overlap function, the observed small production cross-section in $e^+e^- \to b\bar{b}$ was explained. In the tetraquark picture, $Y_b(10890)$ is the $b\bar{b}$ analogue of the $c\bar{c}$ state $Y_c(4260)$, also a P-wave, which is likewise found to have a very small production cross-section, but decays readily into $J/\psi\pi^+\pi^-$. Hence, the two have very similar production and decay characteristics, and, in all likelihood, they have similar compositions.

The current status of $Y_b(10890)$ is unclear. Subsequent to the discovery of $Y_b(10890)$, Belle undertook high-statistics scans for the ratio $R_{b\bar{b}} = \sigma(e^+e^- \to b\bar{b})/\sigma(e^+e^- \to \mu^+\mu^-)$, and also measured more precisely the ratios $R_{\Upsilon(nS)\pi^+\pi^-}$. No results are available on $R_{\Upsilon(nS)\pi^+\pi^-}$ from BaBar, so we discuss the analysis reported by Belle. The two masses, $M(5S)_{b\bar{b}}$ measured through $R_{b\bar{b}}$, and $M(Y_b)$, measured through $R_{\Upsilon(nS)\pi^+\pi^-}$, now differ by slightly more than 2σ, yielding $M(5S)_{b\bar{b}} - M(Y_b) = -9 \pm 4$ MeV. From the mass difference alone, these two could very well be just one and the same state, namely the canonical $\Upsilon(5S)$ - an interpretation adopted by the Belle collaboration[48]. On the other hand, it is now the book keeping of the branching ratios measured at or near the $\Upsilon(5S)$, which is puzzling. This is reflected in the paradox that *direct production* of the $B^{(*)}\bar{B}^{(*)}$ as well as of $B_s\bar{B}_s^{(*)}$ states have essentially no place in the Belle counting[48], as the branching ratios of the $\Upsilon(5S)$ are already saturated by the exotic states ($\Upsilon(nS)\pi^+\pi^-, h_b(mP)\pi^+\pi^-, Z_b(10610)^{\pm}\pi^{\mp}, Z_b(10650)^{\pm}\pi^{\mp}$ and their isospin partners). In our opinion, an interpretation of the Belle data based on two resonances $\Upsilon(5S)$ and $Y_b(10890)$ is more natural, with $\Upsilon(5S)$ having the decays expected for the bottomonium S-state above the $B^{(*)}\bar{B}^{(*)}$ threshold, and the decays of $Y_b(10890)$, a tetraquark, being the source of the exotic states seen. As data taking starts in a couple of years in the form of a new and expanded collaboration, Belle-II, cleaning up the current analysis in the $\Upsilon(5S)$ and $\Upsilon(6S)$ region should be one of their top priorities. In the meanwhile, the 2007 discovery of $Y_b(10890)$ stands, not having been retracted by Belle, at least as far as I know.

Thus, there is a good case that $\Upsilon(5S)$ and $Y_b(10890)$, while having the same $J^{\rm PC} = 1^{--}$ quantum numbers and almost the same mass, are *different* states. As already mesntioned, this is hinted by the drastically different decay characteristics of the dipionic transitions involving the lower quarkonia S-states, such as $\Upsilon(4S) \to \Upsilon(1S)\pi^+\pi^-$, on one hand, and similar decays of the Y_b, on the other. These anomalies are seen both in the decay rates and in the dipion invariant mas spectra in the $\Upsilon(nS)\pi^+\pi^-$

modes. The large branching ratios of $Y_b \to \Upsilon(nS)\pi^+\pi^-$, as well as of $Y(4260) \to J/\psi\pi^+\pi^-$, are due to the Zweig-allowed nature of these transitions, as the initial and final states have the same valence quarks. The final state $\Upsilon(nS)\pi^+\pi^-$ in Y_b decays requires the excitation of a $q\bar{q}$ pair from the vacuum. Since, the light scalars σ_0, $f_0(980)$ are themselves tetraquark candidates[49,50], they are expected to show up in the $\pi^+\pi^-$ invariant mass distributions, as opposed to the corresponding spectrum in the transition $\Upsilon(4S) \to \Upsilon(1S)\pi^+\pi^-$ (see Fig. 4). Subsequent discoveries[51] of the charged states $Z_b^+(10610)$ and $Z_b^+(10650)$, found in the decays $\Upsilon(5s)/Y_b \to Z_b^+(10610)\pi^-, Z_b^+(10650)\pi^-$, leading to the final states $\Upsilon(1S)\pi^+\pi^-$, $\Upsilon(2S)\pi^+\pi^-$, $\Upsilon(3S)\pi^+\pi^-$, $h_b(1P)\pi^+\pi^-$ and $h_b(2P)\pi^+\pi^-$, give credence to the tetraquark interpretation, as discussed below.

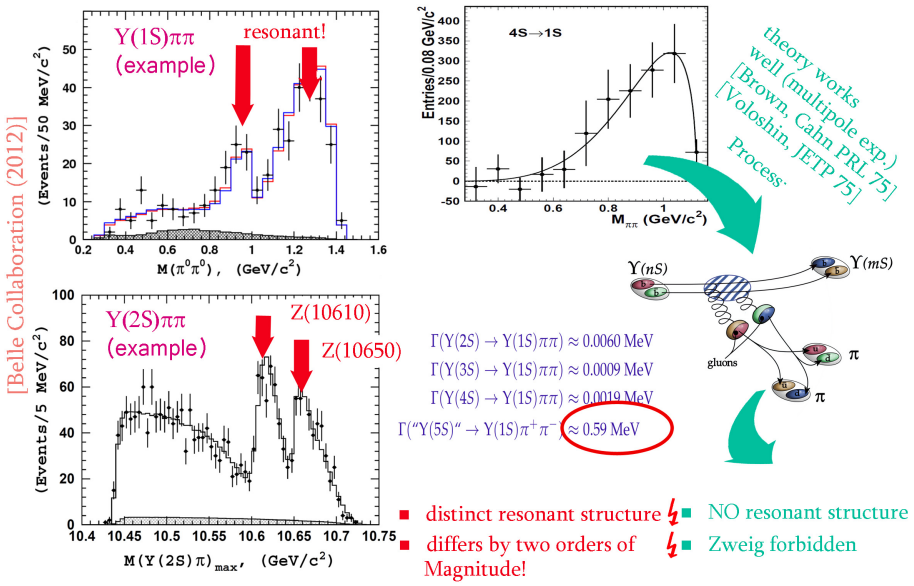

Fig. 4. Dipion invariant mass distribution in $\Upsilon(10890) \to \Upsilon(1S)\pi^0\pi^0$ (upper left frame); the resonances indicated in the dipion spectrum correspond to the $f_0(980)$ and $f_2(1270)$; the resonances $Z(10610)$ and $Z(10650)$ are indicated in the $\Upsilon(2S)\pi^+$ invariant mass distribution from $\Upsilon(10890) \to \Upsilon(2S)\pi^+\pi^-$ (lower left frame). The data are from the Belle collaboration[51]. The upper right hand frame shows the dipion invariant mass distribution in $\Upsilon(4S) \to \Upsilon(1S)\pi^+\pi^-$, and the theoretical curve (with the references) is based on the Zweig-forbidden process shown below. The measured decay widths from $\Upsilon(nS) \to \Upsilon(1S)\pi^+\pi^-$ $nS = 2S, 3S, 4S$ and $\Upsilon(10890) \to \Upsilon(1S)\pi^+\pi^-$ are also shown.This figure serves to underscore the drastically different underlying mechanisms for dipionic transitions in $\Upsilon(nS)$ and $\Upsilon(10890)$ decays.

2.3. *Heavy-Quark-Spin Flip in* $\Upsilon(10890) \to h_b(1P, 2P)\pi\pi$

We summarize the relative rates and strong phases measured by Belle[51] in the process $\Upsilon(10890) \to \Upsilon(nS)\pi^+\pi^-, h_b(mP)\pi^+\pi^-$, with $n = 1, 2, 3$ and $m = 1, 2$ in Table 5. For ease of writing we shall use the notation Z_b and Z_b' for the two charged Z_b states. Here no assumption is made about the nature of $\Upsilon(10890)$, it can be either $\Upsilon(5S)$ or Y_b. Of these, the decay $\Upsilon(10890) \to \Upsilon(1S)\pi^+\pi^-$ involves both a resonant (i.e., via Z/Z') and a direct component, but the other four are dominated by the resonant contribution. One notices that the relative normalizations are very similar and the phases of the $(\Upsilon(2S), \Upsilon(3S))\pi^+\pi^-$ differ by about 180° compared to the ones in $(h_b(1P, h_b(2P))\pi^+\pi^-$. At the first sight this seems to violate the heavy-quark-spin conservation, as in the initial state $s_{b\bar{b}} = 1$, which remains unchanged for the $\Upsilon(nS)$ in the final state, i.e., it involves an $s_{b\bar{b}} = 1 \to s_{b\bar{b}} = 1$ transition, but as $s_{b\bar{b}} = 0$ for the $h_b(mP)$, this involves an $s_{b\bar{b}} = 1 \to s_{b\bar{b}} = 0$ transition, which should have been suppressed, but is not supported by data.

Table 5. Relative normalizations and phases for $s_{b\bar{b}} : 1 \to 1$ and $1 \to 0$ transitions in $\Upsilon(10890)$ decays[51].

Final State	$\Upsilon(1S)\pi^+\pi^-$	$\Upsilon(2S)\pi^+\pi^-$	$\Upsilon(3S)\pi^+\pi^-$	$h_b(1P)\pi^+\pi^-$	$h_b(2P)\pi^+\pi^-$
Rel. Norm.	$0.57 \pm 0.21^{+0.19}_{-0.04}$	$0.86 \pm 0.11^{+0.04}_{-0.10}$	$0.96 \pm 0.14^{+0.08}_{-0.05}$	$1.39 \pm 0.37^{+0.05}_{-0.15}$	$1.6^{+0.6+0.4}_{-0.4-0.6}$
Rel. Phase	$58 \pm 43^{+4}_{-9}$	$-13 \pm 13^{+17}_{-8}$	$-9 \pm 19^{+11}_{-26}$	187^{+44+3}_{-57-12}	$181^{+65+74}_{-105-109}$

It has been shown that this contradiction is only apparent[40]. Expressing the states Z_b and Z_b' in the basis of definite $b\bar{b}$ and light quark $q\bar{q}$ spins, it becomes evident that both the Z_b and Z_b' have $s_{b\bar{b}} = 1$ and $s_{b\bar{b}} = 0$ components,

$$|Z_b\rangle = \frac{|1_{q\bar{q}}, 0_{b\bar{b}}\rangle - |0_{q\bar{q}}, 1_{b\bar{b}}\rangle}{\sqrt{2}}, \quad |Z_b'\rangle = \frac{|1_{q\bar{q}}, 0_{b\bar{b}}\rangle + |0_{q\bar{q}}, 1_{b\bar{b}}\rangle}{\sqrt{2}}.$$

Defining (g is the effective couplings at the vertices $\Upsilon\, Z_b\, \pi$ and $Z_b\, h_b\, \pi$)

$$g_Z \equiv g(\Upsilon \to Z_b\pi)g(Z_b \to h_b\pi) \propto -\alpha\beta\langle h_b|Z_b\rangle\langle Z_b|\Upsilon\rangle,$$
$$g_{Z'} \equiv g(\Upsilon \to Z_b'\pi)g(Z_b' \to h_b\pi) \propto \alpha\beta\langle h_b|Z_b'\rangle\langle Z_b'|\Upsilon\rangle,$$

we note that within errors, Belle data is consistent with the heavy quark spin conservation, which requires $g_Z = -g_{Z'}$. The two-component nature of the Z_b and Z_b' is also the feature which was pointed out earlier for Y_b in the context of the direct transition $Y_b(10890) \to \Upsilon(1S)\pi^+\pi^-$. To determine the coefficients α and β, one has to resort to $s_{b\bar{b}}$: $1 \to 1$ transitions

$$\Upsilon(10890) \to Z_b/Z_b' + \pi \to \Upsilon(nS)\pi\pi \ (n = 1, 2, 3).$$

The analogous effective couplings are

$$f_Z = f(\Upsilon \to Z_b\pi) f(Z_b \to \Upsilon(nS)\pi) \propto |\beta|^2 \langle \Upsilon(nS)|0_{q\bar{q}}, 1_{b\bar{b}}\rangle\langle 0_{q\bar{q}}, 1_{b\bar{b}}|\Upsilon\rangle,$$
$$f_{Z'} = f(\Upsilon \to Z_b'\pi) f(Z_b' \to \Upsilon(nS)\pi) \propto |\alpha|^2 \langle \Upsilon(nS)|0_{q\bar{q}}, 1_{b\bar{b}}\rangle\langle 0_{q\bar{q}}, 1_{b\bar{b}}|\Upsilon\rangle.$$

Dalitz analysis indicates that $\Upsilon(10890) \to Z_b/Z_b' + \pi \to \Upsilon(nS)\pi\pi$ $(n = 1, 2, 3)$ proceed mainly through the resonances Z_b and Z_b', though $\Upsilon(10890) \to \Upsilon(1S)\pi\pi$ has a significant direct component, expected in tetraquark interpretation of $\Upsilon(10890)$ [37]. A comprehensive analysis of the Belle data including the direct and resonant components is required to test the underlying dynamics, which yet to be carried out. However, parametrizing the amplitudes in terms of two Breit-Wigners, one can determine the ratio α/β from $\Upsilon(10890) \to Z_b/Z_b' + \pi \to \Upsilon(nS)\pi\pi$ $(n = 1, 2, 3)$. For the $s_{b\bar{b}} : 1 \to 1$ transition, we get for the averaged quantities:

$$\overline{\text{Rel.Norm.}} = 0.85 \pm 0.08 = |\alpha|^2/|\beta|^2; \quad \overline{\text{Rel.Phase}} = (-8 \pm 10)^\circ.$$

For the $s_{b\bar{b}} : 1 \to 0$ transition, we get

$$\overline{\text{Rel.Norm.}} = 1.4 \pm 0.3; \quad \overline{\text{Rel.Phase}} = (185 \pm 42)^\circ.$$

Within errors, the tetraquark assignment with $\alpha = \beta = 1$ is supported, i.e.,

$$|Z_b\rangle = \frac{|1_{bq}, 0_{\bar{b}\bar{q}}\rangle - |0_{bq}, 1_{\bar{b}\bar{q}}\rangle}{\sqrt{2}}, \quad |Z_b'\rangle = |1_{bq}, 1_{\bar{b}\bar{q}}\rangle_{J=1},$$

and

$$|Z_b\rangle = \frac{|1_{q\bar{q}}, 0_{b\bar{b}}\rangle - |0_{q\bar{q}}, 1_{b\bar{b}}\rangle}{\sqrt{2}}, \quad |Z_b'\rangle = \frac{|1_{q\bar{q}}, 0_{b\bar{b}}\rangle + |0_{q\bar{q}}, 1_{b\bar{b}}\rangle}{\sqrt{2}}.$$

It is interesting that similar conclusion was drawn in the 'molecular' interpretation [52] of the Z_b and Z_b'.

The Fierz rearrangement used in obtaining second of the above relations would put together the $b\bar{q}$ and $q\bar{b}$ fields, yielding

$$|Z_b\rangle = |1_{b\bar{q}}, 1_{\bar{b}q}\rangle_{J=1}, \quad |Z_b'\rangle = \frac{|1_{b\bar{q}}, 0_{q\bar{b}}\rangle + |0_{b\bar{q}}, 1_{q\bar{b}}\rangle}{\sqrt{2}}.$$

Here, the labels $0_{b\bar{q}}$ and $1_{\bar{q}b}$ could be viewed as indicating B and B^* mesons, respectively, leading to the prediction $Z_b \to B^*\bar{B}^*$ and $Z_b' \to B\bar{B}^*$, which is not in agreement with the Belle data[51]. However, this argument rests on the conservation of the light quark spin, for which there is no theoretical foundation. Hence, this last relation is not reliable. Since $Y_b(10890)$ and $\Upsilon(5S)$ are rather close in mass, and there is an issue with the unaccounted *direct production* of the $B^*\bar{B}^*$ and $B\bar{B}^*$ states in the Belle data collected in their vicinity, we conclude that the experimental situation is still in a state of flux and look forward to its resolution with the consolidated Belle-II data.

2.4. *Drell-Yan mechanism for vector exotica production at the LHC and Tevatron*

The exotic hadrons having $J^{\rm PC} = 1^{--}$ can be produced at the Tevatron and LHC via the Drell-Yan process[53] $pp(\bar{p}) \to \gamma^* \to V + ...$ The cases $V = \phi(2170), Y(4260), Y_b(10890)$ have been studied. With the other two hadrons already discussed earlier, we recall that $\phi(2170)$ was first observed in the ISR process $e^+e^- \to \gamma_{\rm ISR} f_0(980)\phi(1020)$ by BaBaR[54] and later confirmed by BESII[55] and Belle[56]. Drenska *et al.*[57] interpreted $\phi(1270)$ as a P-wave tetraquark $[sq][\bar{s}\bar{q}]$. Thus, all three vector exotica are assumed to be the first orbital excitation of diquark-antidiquark states with a hidden $s\bar{s}$, $c\bar{c}$ and $b\bar{b}$ quark content, respectively. As all three have very small branching ratios in a dilepton pair, they should be searched for in the decay modes in which they have been discovered, and these are $\phi(2170) \to f_0(980)\phi(1020) \to \pi^+\pi^-K^+K^-$, $Y(4260) \to J/\psi\pi^+\pi^- \to \mu^+\mu^-\pi^+\pi^-$ and $Y_b(10890) \to \Upsilon(nS)\pi^+\pi^- \to \mu^+\mu^-\pi^+\pi^-$. Thus, they involve four charged particles, which can be detected at hadron colliders. With their masses, total and partial decay widths taken from the PDG[58], the cross sections for the processes $p\bar{p}(p) \to \phi(2170)(\to \phi(1020)f_0(980) \to K^+K^-\pi^+\pi^-)$, $p\bar{p}(p) \to Y(4260)(\to J/\psi\pi^+\pi^- \to \mu^+\mu^-\pi^+\pi^-)$, and $p\bar{p}(p) \to Y_b(10890)(\to \Upsilon(1S, 2S, 3S)\pi^+\pi^- \to \mu^+\mu^-\pi^+\pi^-)$, at the Tevatron ($\sqrt{s} = 1.96$ TeV) and the LHC are given in Table 6, with the indicated rapidity ranges. All these processes have measurable rates, and they should be searched for, in particular, at the LHC.

Summarizing this discussion, we note that there are several puzzles in the X, Y, Z sector. These involve the nature of the $J^{PC} = 1^{--}$ states, $Y(4260)$ and $Y(10890)$, and whether they are related with each other. Also, whether $Y(10890)$ and $\Upsilon(5S)$ are one and the same particle is still an open

Table 6. Cross sections (in units of pb) for the processes $p\bar{p}(p) \to \phi(2170)(\to \phi(1020) f_0(980) \to K^+K^-\pi^+\pi^-)$, $p\bar{p}(p) \to Y(4260)(\to J/\psi\pi^+\pi^- \to \mu^+\mu^-\pi^+\pi^-)$, and $p\bar{p}(p) \to Y_b(10890)(\to \Upsilon(1S,2S,3S)\pi^+\pi^- \to \mu^+\mu^-\pi^+\pi^-)$, at the Tevatron ($\sqrt{s} = 1.96$ TeV) and the LHC[53].

	$\phi(2170)$	$Y(4260)$	$Y_b(10890)$
Tevatron($\|y\| < 2.5$)	$2.3^{+0.9}_{-0.9}$	$0.23^{+0.19}_{-0.05}$	$0.0020^{+0.0006}_{-0.0005}$
LHC 7TeV ($\|y\| < 2.5$)	$3.6^{+1.4}_{-1.4}$	$0.40^{+0.32}_{-0.09}$	$0.0040^{+0.0013}_{-0.0011}$
LHCb 7TeV ($1.9 < y < 4.9$)	$2.2^{+1.2}_{-1.1}$	$0.24^{+0.20}_{-0.07}$	$0.0023^{+0.0007}_{-0.0006}$
LHC 14TeV ($\|y\| < 2.5$)	$4.5^{+1.9}_{-1.9}$	$0.54^{+0.44}_{-0.12}$	$0.0060^{+0.0019}_{-0.0016}$
LHCb 14TeV ($1.9 < y < 4.9$)	$2.7^{+1.9}_{-1.6}$	$0.31^{+0.27}_{-0.11}$	$0.0033^{+0.0011}_{-0.0010}$

issue. In principle, both $Y(4260)$ and $Y(10890)$ can be produced at the LHC and measured through the $J\psi\pi^+\pi^-$ and $\Upsilon(nS)\pi^+\pi^-$ ($nS = 1S, 2S, 3S$) modes, respectively. Their hadroproduction cross-sections are unfortunately uncertain, but their (normalized) transverse momentum distributions will be quite revealing. As they are both $J^{PC} = 1^{--}$ hadrons, they can also be produced via the Drell-Yan mechanism and detected through their signature decay modes. We have argued that the tetraquark interpretation of the charged exotics Z_b and Z_b' leads to a straight forward understanding of the relative rates and strong phases of the heavy quark spin non-flip and spin-flip transitions in the decays $\Upsilon(10890) \to \Upsilon(nS)\pi^+\pi^-$ and $\Upsilon(10890) \to h_b(mP)\pi^+\pi^-$, respectively. In the tetraquark picture, the corresponding hadrons in the charm sector Z_c and Z_c' are related to their $b\bar{b}$ counterparts. We look forward to the higher luminosity data at Bell-II and LHC to resolve some of these issues.

3. Pentaquarks

Pentaquarks remained cursed for almost a decade under the shadow of the botched discoveries of $\Theta(1540)$, $\Phi(1860)$, $\Theta_c(3100)$. The sentiment of the particle physics community is reflected in the terse 2014 PDG review[59]:
There are two or three recent experiments that find weak evidence for signals near the nominal masses, but there is simply no point in tabulating them in view of the overwhelming evidence that the claimed pentaquarks do not exist. The only advance in particle physics thought worthy of mention in the American Institute of Physics "Physics News in 2003" was a false alarm.

The whole story — is a curious episode in the history of science.

This seems to have changed by the observation of $J/\psi p$ resonances consistent with pentaquark states in $\Lambda_b^0 \to J/\psi K^- p$ decays by the LHCb collaboration[60]. The discovery channel ($\sqrt{s}$ = 7 and 8 TeV, $\int Ldt$ = 3 fb^{-1}) is

$$pp \to b\bar{b} \to \Lambda_b X; \Lambda_b \to K^- J/\psi p.$$

A statistically good fit of the $m_{J/\psi p}$-distribution is consistent with the presence of two resonant states, henceforth called $P_c(4450)^+$ and $P_c(4380)^+$, with the following characteristics

$$M = 4449.8 \pm 1.7 \pm 2.5 \text{ MeV}; \quad \Gamma = 39 \pm 5 \pm 19 \text{ MeV},$$

and

$$M = 4380 \pm 8 \pm 29 \text{ MeV}; \quad \Gamma = 205 \pm 18 \pm 86 \text{ MeV},$$

having the statistical significance of 12σ and 9σ, respectively. Both of them carry a unit of baryonic number and have the valence quarks $P_c^+ = \bar{c}cuud$. The preferred $J^{\rm P}$ assignments are $5/2^+$ for the $P_c(4450)^+$ and $3/2^-$ for the $P_c(4380)^+$. Doing an Argand-diagram analysis in the (Im A^{P_c} - Re A^{P_c}) plane, the phase change in the amplitude is consistent with a resonance for the $P_c(4450)^+$, but less so for the $P_c(4380)^+$.

Following a pattern seen for the tetraquark candidates, namely their proximity to respective thresholds, such as $D\bar{D}^*$ for the $X(3872)$, $B\bar{B}^*$ and $B^*\bar{B}^*$ for the $Z_b(10610)$ and $Z_b(10650)$, respectively, also the two pentaquark candidates $P_c(4380)$ and $P_c(4450)$ lie close to several charm meson-baryon thresholds[61]. The $\Sigma_c^{*+}\bar{D}^0$ has a threshold of 4382.3 ± 2.4 MeV, tantalizingly close to the mass of $P_c(4380)^+$. In the case of $P_c(4450)^+$, there are several thresholds within striking distance, $\chi_{c1}p(4448.93 \pm 0.07)$, $\Lambda_c^{*+}\bar{D}^0(4457.09 \pm 0.35)$, $\Sigma_c^+\bar{D}^{*0}(4459.9 \pm 0.9)$, and $\Sigma_c^+\bar{D}^0\pi^0(4452.7 \pm 0.5)$, where the masses are in units of MeV. This has led to a number of hypotheses to accommodate the two P_c states, which can be classified under four different mechanisms:

- Rescattering-induced kinematic effects[62–65].
- $P_c(4380)$ and $P_c(4450)$ as baryocharmonia[66].
- Open charm-baryons and charm-meson bound states[67–71].
- Compact pentaquarks[72–79]

We discuss the first three briefly and the compact pentaquarks in somewhat more detail subsequently.

Kinematic effects can result in a narrow structure around the $\chi_{c1}p$ threshold. Two possible mechanisms shown in Fig. 5 are:
(a) 2-point loop with a 3-body production $\Lambda_b^0 \to K^-\,\chi_{c1}\,p$ followed by the

rescattering process $\chi_{c1}\, p \to J/\psi\, p$, and
(b) in which $K^-\, p$ is produced from an intermediate Λ^* and the proton rescatters with the χ_{c1} into a $J/\psi\, p$, as shown below.

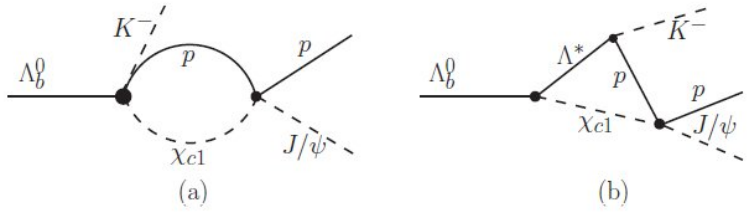

Fig. 5. The two scattering diagrams discussed in the text [62].

In the baryocharmonium picture, the P_c states are hadroquarkonium-type composites of J/ψ and excited nucleon states similar to the known resonances $N(1440)$ and $N(1520)$. Photoproduction of the P_c states in $\gamma + p$ collisions is advocated as sensitive probe of this mechanism [66].

In the hadronic molecular interpretation, one identifies $P_c(4380)^+$ with $\Sigma_c(2455)\bar{D}^*$ and $P_c(4450)^+$ with $\Sigma_c(2520)\bar{D}^*$, which are bound by a pion exchange. This can be expressed in terms of the effective Lagrangians:

$$\mathcal{L}_{\mathcal{P}} = ig\mathrm{Tr}\left[\bar{H}_a^{(\bar{Q})}\,\gamma^\mu\, A^\mu_{ab}\,\gamma_5 H_b^{(\bar{Q})}\right],$$
$$\mathcal{L}_{\mathcal{S}} = -\frac{3}{2} g_1 \epsilon^{\mu\lambda\nu\kappa} v_\kappa \mathrm{Tr}\left[\bar{\mathcal{S}}_\mu\, A_\nu\, \mathcal{S}_\lambda\right].$$

Here $H_a^{(\bar{Q})} = [P_a^{*(\bar{Q})\,\mu}\gamma_\mu - P_a^{(\bar{Q})}\gamma_5](1-\not{v})/2$ is a pseudoscalar and vector charmed meson multiplet (D, D^*), v being the four-velocity vector $v = (0, \vec{1})$, $\mathcal{S}_\mu = 1/\sqrt{3}(\gamma_\mu + v_\mu)\gamma^5\mathcal{B}_6 + \mathcal{B}^*_{6\mu}$ stands for the charmed baryon multiplet, with $\mathcal{B}_6$ and $\mathcal{B}^*_{6\mu}$ corresponding to the $J^P = 1/2^+$ and $J^P = 3/2^+$ in 6_F flavor representation, respectively, and A_μ is an axial-vector current, containing a pion chiral multiplet. This interaction lagrangian is used to work out effective potentials, energy levels and wave-functions of the $\Sigma_c^{(*)}\bar{D}^*$ systems. In this picture, $P_c(4380)^+$ is a $\Sigma_c\bar{D}^*$ ($I = 1/2$, $J = 3/2$) molecule, and $P_c(4450)^+$ is a $\Sigma_c^*\bar{D}^*$ ($I = 1/2$, $J = 5/2$) molecule. Apart from accommodating the two observed pentaquarks, this framework predicts two additional hidden-charm molecular pentaquark states, $\Sigma_c\bar{D}^*$ ($I = 3/2$, $J = 1/2$) and $\Sigma_c^*\bar{D}^*$ ($I = 3/2$, $J = 1/2$), which are isospin partners of $P_c(4380)^+$ and $P_c(4450)^+$, respectively, decaying into $\Delta(1232)J/\psi$ and $\Delta(1232)\eta_c$. In addition, a rich pentaquark spectrum of

states for the hidden-bottom $(\Sigma_b B^*, \Sigma_b^* B^*)$, B_c-like $(\Sigma_c B^*, \Sigma_c^* B^*)$ and $(\Sigma_b \bar{D}^*, \Sigma_b^* \bar{D}^*)$ with well-defined (I, J) are predicted.

3.1. $P_c(4380)^+$ and $P_c(4450)^+$ as compact pentaquarks

This hypothesis has been put forward in a number of papers; to be specific we shall concentrate here on the description by Maiani *et al.*[72], in which the two P_c states (also denoted by the symbols $\mathbb{P}^+(3/2^-)$ and $\mathbb{P}^+(5/2^+)$) have the valence structure diquark-diquark-antiquark, as shown schematically in Fig. 6 below. The assumed assignments are[72]:

$$P_c(4380)^+ = \mathbb{P}^+(3/2^-) = \{\bar{c}\,[cq]_{s=1}[q'q'']_{s=1}, L = 0\}\,,$$
$$P_c(4450)^+ = \mathbb{P}^+(5/2^+) = \{\bar{c}\,[cq]_{s=1}[q'q'']_{s=0}, L = 1\}\,.$$

The observed mass difference $P_c(4450)^+ - P_c(4380)^+ \simeq 70$ MeV is accounted for as follows: The level spacing for $\Delta L = 1$ is set using the light baryons $\Lambda(1405) - \Lambda(1116) \sim 290$ MeV. The light-light diquark $[q'q'']$ spin-dependent mass difference $(\Delta S = 1)$ is determined from the diquark-quark interpretation of the charm baryons $[qq']_{s=1} - [qq']_{s=0} = \Sigma_c(2455) - \Lambda_c(2286) \simeq 170$ MeV. Thus, the orbital mass gap $\mathbb{P}^+(3/2^-) - \mathbb{P}^+(5/2^+)$ is thereby reduced to 120 MeV, in approximate agreement with the data.

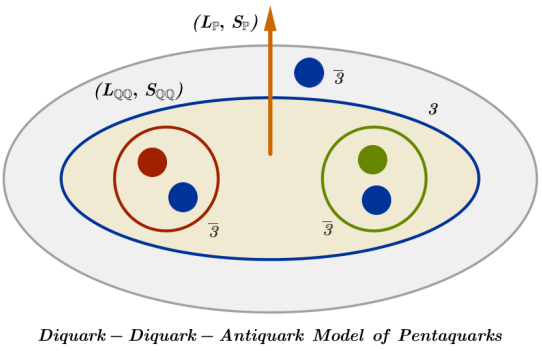

Fig. 6.

Two possible mechanisms of pentaquark production in $\Lambda_b^0 \to K^- J/\psi p$ have been proposed[72]. In the first, the b-quark spin is shared between the K^-, the $\bar{c}$ and the $[cu]$ components, and the $[ud]$ diquark in the final state retains its spin, i.e. it has spin-0, (Fig. 7 A below). This is the decay mechanism compatible with heavy-quark-spin conservation, which implies that the spin of the light diquark in Λ_b^0 decay is also conserved. In

the second, the $[ud]$ diquark is formed from the original d quark, and the u quark from the vacuum $u\bar{u}$. In this case, angular momentum is shared among all components, and the diquark $[ud]$ may have both spins, $s = 0, 1$ (Fig. 7 B below). Which of the two diagrams dominate is a dynamical question; entries in the PDG on the decays of Λ_b hint that the mechanism in Fig. B is dynamically suppressed, as also anticipated by the heavy-quark-spin conservation.

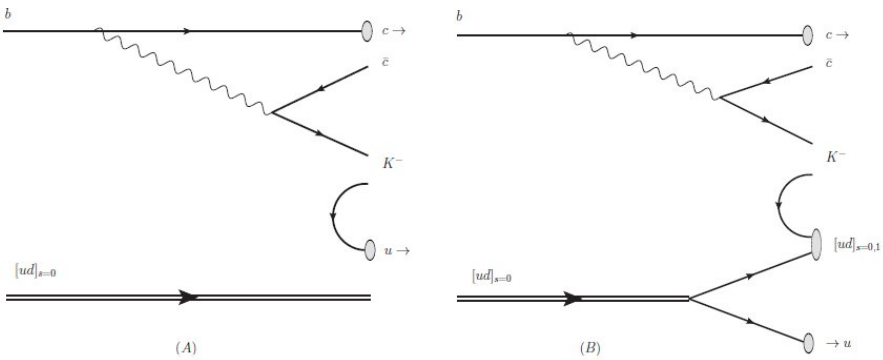

Fig. 7. Two mechanisms for the decays $\Lambda_b^0 \to J/\psi K^- p$ in the pentaquark picture[72].

3.2. $SU(3)_F$ structure of pentaquarks

Concentrating on the quark flavor of the pentaquarks $\mathbb{P}_c^+ = \bar{c}cuud$, they are of two different types:

$$\mathbb{P}_u = \epsilon^{\alpha\beta\gamma}\bar{c}_\alpha\,[cu]_{\beta,s=0,1}\,[ud]_{\gamma,s=0,1},$$
$$\mathbb{P}_d = \epsilon^{\alpha\beta\gamma}\bar{c}_\alpha\,[cd]_{\beta,s=0,1}\,[uu]_{\gamma,s=1},$$

the difference being that the $\mathbb{P}_d$ involves a $[uu]$ diquark, and the Pauli exclusion principle implies that this diquark has to be in an $SU(3)_F$-symmetric representation. This leads to two distinct $SU(3)_F$ series of pentaquarks

$$\mathbb{P}_A = \epsilon^{\alpha\beta\gamma}\,\{\bar{c}_\alpha\,[cq]_{\beta,s=0,1}\,[q'q'']_{\gamma,s=0}, L\} = \mathbf{3}\otimes\bar{\mathbf{3}} = \mathbf{1}\oplus\mathbf{8},$$
$$\mathbb{P}_S = \epsilon^{\alpha\beta\gamma}\,\{\bar{c}_\alpha\,[cq]_{\beta,s=0,1}\,[q'q'']_{\gamma,s=1}, L\} = \mathbf{3}\otimes\mathbf{6} = \mathbf{8}\oplus\mathbf{10}.$$

For S waves, the first and the second series have the angular momenta

$$\mathbb{P}_A(L=0): \quad J = 1/2(2),\ 3/2(1),$$
$$\mathbb{P}_S(L=0): \quad J = 1/2(3),\ 3/2(3),\ 5/2(1),$$

where the multiplicities are given in parentheses. One assigns $\mathbb{P}(3/2^-)$ to the $\mathbb{P}_A$ and $\mathbb{P}(5/2^+)$ to the $\mathbb{P}_S$ series of pentaquarks[72].

The $SU(3)_F$ based analysis of the decays $\Lambda_b \to \mathbb{P}^+ K^- \to (J/\psi\, p)K^-$ goes as follows. With respect to $SU(3)_F$, $\Lambda_b(bud) \sim \bar{3}$ and it is an isosinglet $I = 0$. Thus, the weak non-leptonic Hamiltonian for $b \to c\bar{c}s$ decays is:

$$H^{(3)}_{\rm eff}(\Delta I = 0, \Delta S = -1).$$

The explicit form of the weak Hamiltonian is given by

$$H^{(3)}_{\rm eff} = \frac{G_F}{\sqrt{2}}[V_{cb}V^*_{cs}(c_1 O_1 + c_2 O_2)],$$

where G_F is the Fermi coupling constant, V_{cs} is the CKM matrix element, c_1 and c_2 are the Wilson coefficients of the operators O_1 and O_2, respectively, with the operators defined as (i, j are color indices)

$$O_1 = (\bar{s}_i c_j)_{V-A}(\bar{c}_i b_j)_{V-A}, \quad O_2 = (\bar{s}c)_{V-A}(\bar{c}b)_{V-A},$$

and the penguin amplitudes are ignored. With M a nonet of $SU(3)$ light mesons (π, K, η, η'), the weak transitions $\langle \mathbb{P}, M|H_{\rm W}|\Lambda_b\rangle$ requires $\mathbb{P} + M$ to be in $8 \oplus 1$ representation. Recalling the $SU(3)$ group multiplication rule

$$\begin{aligned} 8 \otimes 8 &= 1 \oplus 8 \oplus 8 \oplus 10 \oplus \bar{10} \oplus 27, \\ 8 \otimes 10 &= 8 \oplus 10 \oplus 27 \oplus 35, \end{aligned}$$

the decay $\langle \mathbb{P}, M|H_{\rm W}|\Lambda_b\rangle$ can be realized with $\mathbb{P}$ in either an octet `8` or a decuplet `10`. The discovery channel $\Lambda_b \to \mathbb{P}^+ K^- \to J/\psi p K^-$ corresponds to $\mathbb{P}$ in an octet `8`.

3.3. *Weak decays with $\mathbb{P}$ in Decuplet representation*

Decays involving the decuplet `10` pentaquarks may also occur, if the light diquark pair having spin-0 $[ud]_{s=0}$ in Λ_b gets broken to produce a spin-1 light diquark $[ud]_{s=1}$. In this case, one would also observe the decays of Λ_b, such as

$$\begin{aligned} \Lambda_b &\to \pi \mathbb{P}^{(S=-1)}_{10} \to \pi(J/\psi\Sigma(1385)), \\ \Lambda_b &\to K^+ \mathbb{P}^{(S=-2)}_{10} \to K^+(J/\psi\Xi^-(1530)). \end{aligned}$$

These decays are, however, disfavored by the heavy-quark-spin-conservation selection rules. The extent to which this rule is compatible with the existing data on B-meson and Λ_b decays can be seen in the PDG entries. Whether the decays of the pentaquarks are also subject to the same selection rules

is yet to be checked, but on symmetry grounds, we do expect it to hold. Hence, the observation (or not) of these decays will be quite instructive.

Apart from $\Lambda_b(bud)$, several other b-baryons, such as $\Xi_b^0(usb)$, $\Xi_b^-(dsb)$ and $\Omega_b^-(ssb)$ undergo weak decays. These b-baryons are characterized by the spin of the light diquark, as shown below, making their isospin (I) and strangeness (S) quantum numbers explicit as well as their light diquark $j^{\rm P}$ quantum numbers. The c-baryons are likewise characterized similarly.

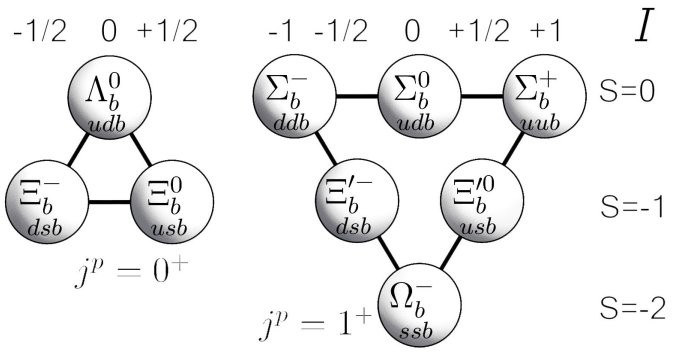

Fig. 8. b-baryons with the light diquark spins $j^p = 0^+$ (left) and $j^p = 1^+$ (right).

Examples of bottom-strange b-baryon in various charge combinations, respecting $\Delta I = 0$, $\Delta S = -1$ are:

$$\Xi_b^0(5794) \to K(J/\psi\Sigma(1385)),$$

which corresponds to the formation of the pentaquarks with the spin configuration $\mathbb{P}_{10}(\bar{c}\,[cq]_{s=0,1}\,[q's]_{s=0,1})$ with $(q, q' = u, d)$.
Above considerations have been extended involving the entire $SU(3)_F$ multiplets entering the generic decay amplitude $\langle \mathcal{P}\mathcal{M}|H_{\rm eff}|\mathcal{B}\rangle$, where $\mathcal{B}$ is the $SU(3)_F$ antitriplet b-baryon, shown in the left frame of Fig. 8, $\mathcal{M}$ is the 3×3 pseudoscalar meson matrix

$$\mathcal{M}_i^j = \begin{pmatrix} \frac{\pi^0}{\sqrt{2}} + \frac{\eta_8}{\sqrt{6}} & \pi^+ & K^+ \\ \pi^- & -\frac{\pi^0}{\sqrt{2}} + \frac{\eta_8}{\sqrt{6}} & K^0 \\ K^- & \bar{K}^0 & -\frac{2\eta_8}{\sqrt{6}} \end{pmatrix},$$

and $\mathcal{P}$ is a pentaquark state belonging to an octet with definite J^P, denoted as a 3×3 matrix J^P, $\mathcal{P}_j^i(J^{\rm P})$,

$$\mathcal{P}_i^j\left(J^P\right)=\begin{pmatrix}\frac{P_{\Sigma^0}}{\sqrt{2}}+\frac{P_\Lambda}{\sqrt{6}} & P_{\Sigma^+} & P_p\\ P_{\Sigma^-} & -\frac{P_{\Sigma^0}}{\sqrt{2}}+\frac{P_\Lambda}{\sqrt{6}} & P_n\\ P_{\Xi^-} & P_{\Xi^0} & -\frac{P_\Lambda}{\sqrt{6}}\end{pmatrix},$$

or a decuplet $\mathcal{P}_{ijk}$ (symmetric in the indices), with $\mathcal{P}_{111}=\Delta_{10}^{++},...,\mathcal{P}_{333}=\Omega_{10}^{-}$. (see Guan-Nan Li *et al.*[74] for a detailed list of the component fields and $SU(3)_F$-based relations among decay widths). The two observed pentaquarks are denoted as $P_p(3/2^-)$ and $P_p(5/2^+)$. Estimates of the $SU(3)$ amplitudes require a dynamical model, which will be lot more complex to develop than the factorization-based models for the two-body B-meson decays, but, as argued in the literature, SU(3) symmetry can be used to relate different decay modes.

Examples of the weak decays in which the initial b-baryon has a spin-1 light diquark, i.e. $j^{\rm P}=1^+$, which is retained in the transition, are provided by the Ω_b decays. The $s\bar{s}$ pair in Ω_b is in the symmetric $\mathtt{6}$ representation of $SU(3)_F$ with spin 1 and is expected to produce decuplet pentaquarks in association with a ϕ or a Kaon[72]

$$\Omega_b(6049)\to\phi(J/\psi\,\Omega^-(1672)),K(J/\psi\,\Xi(1387)).$$

These correspond, respectively, to the formation of the following pentaquarks ($q=u,\,d$)

$$\mathbb{P}_{10}^{-}(\bar{c}\,[cs]_{s=0,1}\,[ss]_{s=1}),\mathbb{P}_{10}(\bar{c}\,[cq]_{s=0,1}\,[ss]_{s=1}).$$

These transitions are expected on firmer theoretical footings, as the initial $[ss]$ diquark in Ω_b is left unbroken. Again, lot more transitions can be found relaxing this condition, which would involve a $j^{\rm P}=1^+\to 0^+$ light diquark, but they are anticipated to be suppressed.

In summary, with the discoveries of the X,Y,Z and P_c states a new era of hadron spectroscopy has dawned. In addition to the well-known $q\bar{q}$ mesons and qqq baryons, we have convincing evidence that the hadronic world is multi-layered, in the form of tetraquark mesons, pentaquark baryons, and likely also the hexaquarks (or H dibaryons)[80]. However, the underlying dynamics is far from being understood. It has taken almost fifty years since the advent of QCD to develop quantitative understanding of the conventional hadronic physics. A very long road lies ahead of us before we can realistically expect to achieve a comparable understanding of multiquark hadrons. Existence proof of tetra- and pentaquarks on the lattice would be a breakthrough. In the meanwhile, phenomenological models built within constrained theoretical frameworks are unavoidable. They and

experiments will guide us how to navigate through this uncharted territory. The case of diquark models in this context was reviewed here. More data and poweful theoretical techniques are needed to make further progress on this front.

4. Acknowledgements

I would like to thank the organizers of the 14th. regional meeting on mathematical physics in Islamabad, in particular, M. Jamil Aslam and Khalid Saifullah, for inviting me and for their warm hospitality. Generous travel support offered by Dr. Shaukat Hameed Khan and COMSTECH, Islamabad, is also gratefully acknowledged.

References

1. S.-K. Choi *et al.* (Belle Collaboration), Phys. Rev. Lett. **91**, 262001 (2003).
2. H. X. Chen, W. Chen, X. Liu and S. L. Zhu, arXiv:1601.02092 [hep-ph].
3. S. L. Olsen, PoS Bormio 050 (2015) [arXiv:1511.01589 [hep-ex]].
4. R. A. Briceno *et al.*, Chin. Phys. C **40** (2016) no.4, 042001 [arXiv:1511.06779 [hep-ph]].
5. A. Esposito, A. L. Guerrieri, F. Piccinini, A. Pilloni and A. D. Polosa, Int. J. Mod. Phys. A **30**, 1530002 (2015) [arXiv:1411.5997 [hep-ph]].
6. G. T. Bodwin, E. Braaten, E. Eichten, S. L. Olsen, T. K. Pedlar and J. Russ, arXiv:1307.7425.
7. E. S. Swanson, arXiv:1504.07952 [hep-ph].
8. E. S. Swanson, Phys. Rev. D **91** (2015) no.3, 034009 [arXiv:1409.3291 [hep-ph]].
9. S. Dubynskiy and M. B. Voloshin, Phys. Lett. B **666**, 344 (2008) [arXiv:0803.2224 [hep-ph]].
10. F. E. Close and P. R. Page, Nucl. Phys. B **443**, 233 (1995) [hep-ph/9411301].
11. F. E. Close and P. R. Page, Phys. Lett. B **628**, 215 (2005) [hep-ph/0507199].
12. E. Kou and O. Pene, Phys. Lett. B **631**, 164 (2005) [hep-ph/0507119].
13. S. L. Zhu, Phys. Lett. B **625**, 212 (2005) [hep-ph/0507025].
14. C. A. Meyer and E. S. Swanson, Prog. Part. Nucl. Phys. **82**, 21 (2015) [arXiv:1502.07276 [hep-ph]].
15. M. R. Pennington, EPJ Web Conf. **113** (2016) 01014 [arXiv:1509.02555 [nucl-th]].

16. N. A. Tornqvist, Z. Phys. C **61**, 525 (1994) [hep-ph/9310247]; E. Braaten and M. Kusunoki, Phys. Rev. D **69**, 074005 (2004) [hep-ph/0311147]; F. E. Close and P. R. Page, Phys. Lett. B **578**, 119 (2004) [hep-ph/0309253]; E. S. Swanson, Phys. Rept. **429**, 243 (2006) [hep-ph/0601110]; M. Cleven, F. K. Guo, C. Hanhart and U. G. Meissner, Eur. Phys. J. A **47**, 120 (2011) [arXiv:1107.0254 [hep-ph]].
17. C. Bignamini, B. Grinstein, F. Piccinini, A. D. Polosa and C. Sabelli, Phys. Rev. Lett. **103**, 162001 (2009) [arXiv:0906.0882 [hep-ph]].
18. P. Artoisenet and E. Braaten, Phys. Rev. D **81**, 114018 (2010) [arXiv:0911.2016 [hep-ph]].
19. T. Gutsche, M. Kesenheimer and V. E. Lyubovitskij, Phys. Rev. D **90**, no. 9, 094013 (2014) [arXiv:1410.0259 [hep-ph]].
20. M. Cleven, arXiv:1405.4195 [hep-ph].
21. F.-K. Guo, C. Hanhart, Y. S. Kalashnikova, P. Matuschek, R. V. Mizuk, A. V. Nefediev, Q. Wang and J.-L. Wynen, Phys. Rev. D **93**, no. 7, 074031 (2016) [arXiv:1602.00940 [hep-ph]].
22. P. Artoisenet, E. Braaten and D. Kang, Phys. Rev. D **82**, 014013 (2010) [arXiv:1005.2167 [hep-ph]].
23. C. Hanhart, Y. S. Kalashnikova and A. V. Nefediev, Eur. Phys. J. A **47**, 101 (2011) [arXiv:1106.1185 [hep-ph]].
24. C. Meng, J. J. Sanz-Cillero, M. Shi, D. L. Yao and H. Q. Zheng, Phys. Rev. D **92**, no. 3, 034020 (2015) [arXiv:1411.3106 [hep-ph]].
25. T. Barnes, F. E. Close and E. S. Swanson, Phys. Rev. D **91**, no. 1, 014004 (2015) [arXiv:1409.6651 [hep-ph]].
26. L. Maiani, F. Piccinini, A. D. Polosa and V. Riquer, Phys. Rev. Lett. **93** (2004) 212002 [hep-ph/0407017].
27. L. Maiani, F. Piccinini, A. D. Polosa and V. Riquer, Phys. Rev. D **71**, 014028 (2005) [hep-ph/0412098].
28. S. J. Brodsky, D. S. Hwang and R. F. Lebed, Phys. Rev. Lett. **113**, no. 11, 112001 (2014) [arXiv:1406.7281 [hep-ph]].
29. S. Weinberg, Phys. Rev. Lett. **110**, 261601 (2013) [arXiv:1303.0342 [hep-ph]].
30. M. Knecht and S. Peris, Phys. Rev. D **88**, 036016 (2013) [arXiv:1307.1273 [hep-ph]].
31. G. Rossi and G. Veneziano, arXiv:1603.05830 [hep-th].
32. M. Padmanath, C. B. Lang and S. Prelovsek, arXiv:1510.09150 [hep-lat].
33. C. DeTar, arXiv:1511.06884 [hep-lat].
34. L. Maiani, F. Piccinini, A. D. Polosa and V. Riquer, Phys. Rev. D **89**,

114010 (2014) [arXiv:1405.1551 [hep-ph]].
35. A. Ali, C. Hambrock, I. Ahmed and M. J. Aslam, Phys. Lett. B **684**, 28 (2010) [arXiv:0911.2787 [hep-ph]].
36. A. Ali, C. Hambrock and M. J. Aslam, Phys. Rev. Lett. **104**, 162001 (2010) Erratum: [Phys. Rev. Lett. **107**, 049903 (2011)] [arXiv:0912.5016 [hep-ph]].
37. A. Ali, C. Hambrock and S. Mishima, Phys. Rev. Lett. **106**, 092002 (2011) [arXiv:1011.4856 [hep-ph]].
38. C. Alexandrou, P. de Forcrand and B. Lucini, Phys. Rev. Lett. **97**, 222002 (2006) [hep-lat/0609004].
39. R. L. Jaffe, Phys. Rept. **409**, 1 (2005) [hep-ph/0409065].
40. A. Ali, L. Maiani, A. D. Polosa and V. Riquer, Phys. Rev. D **91**, no. 1, 017502 (2015) [arXiv:1412.2049 [hep-ph]].
41. D. Ebert, R. N. Faustov and V. O. Galkin, Phys. Lett. B **634**, 214 (2006) [hep-ph/0512230].
42. A. Ali, L. Maiani, A. D. Polosa and V. Riquer, arXiv:1604.01731 [hep-ph].
43. V. M. Abazov *et al.* [D0 Collaboration], [arXiv:1602.07588 [hep-ex]].
44. The LHCb Collaboration [LHCb Collaboration], LHCb-CONF-2016-004, CERN-LHCb-CONF-2016-004.
45. S. S. Agaev, K. Azizi and H. Sundu, arXiv:1603.02708 [hep-ph].
46. K. F. Chen *et al.* [Belle Collaboration], Phys. Rev. Lett. **100**, 112001 (2008) [arXiv:0710.2577 [hep-ex]].
47. N. Brambilla *et al.*, Eur. Phys. J. C **71**, 1534 (2011) [arXiv:1010.5827 [hep-ph]].
48. D. Santel *et al.* [Belle Collaboration], Phys. Rev. D **93** (2016) no.1, 011101 [arXiv:1501.01137 [hep-ex]].
49. G. 't Hooft, G. Isidori, L. Maiani, A. D. Polosa and V. Riquer, Phys. Lett. B **662**, 424 (2008) [arXiv:0801.2288 [hep-ph]].
50. A. H. Fariborz, R. Jora and J. Schechter, Phys. Rev. D **77**, 094004 (2008) [arXiv:0801.2552 [hep-ph]].
51. A. Bondar *et al.* [Belle Collaboration], Phys. Rev. Lett. **108**, 122001 (2012) doi:10.1103/PhysRevLett.108.122001 [arXiv:1110.2251 [hep-ex]].
52. A. E. Bondar *et al.*, Phys. Rev. D **84**, 054010 (2011) [arXiv:1105.4473 [hep-ph]].
53. A. Ali and W. Wang, Phys. Rev. Lett. **106**, 192001 (2011) [arXiv:1103.4587 [hep-ph]].
54. B. Aubert *et al.* [BaBar Collaboration], Phys. Rev. D **74**, 091103 (2006)

[hep-ex/0610018].
55. M. Ablikim *et al.* [BES Collaboration], Phys. Rev. Lett. **100**, 102003 (2008) [arXiv:0712.1143 [hep-ex]].
56. C. P. Shen *et al.* [Belle Collaboration], Phys. Rev. D **80**, 031101 (2009) doi:10.1103/PhysRevD.80.031101 [arXiv:0808.0006 [hep-ex]].
57. N. V. Drenska, R. Faccini and A. D. Polosa, Phys. Lett. B **669**, 160 (2008) [arXiv:0807.0593 [hep-ph]].
58. K.A. Olive *et al.* (Particle Data Group), Chinese Phys., **C 38**, 090001 (2014).
59. See the review by G. C.Wohl in K.A. Olive *et al.* (Particle Data Group), Chinese Phys.,**C 38**, 090001 (2014).
60. R. Aaij *et al.* [LHCb Collaboration], Phys. Rev. Lett. **115** (2015) 072001 [arXiv:1507.03414 [hep-ex]].
61. T. J. Burns, Eur. Phys. J. A **51** (2015) no.11, 152 [arXiv:1509.02460 [hep-ph]].
62. F. K. Guo, U. G. Meiner, W. Wang and Z. Yang, Phys. Rev. D **92**, no. 7, 071502 (2015) [arXiv:1507.04950 [hep-ph]].
63. X. H. Liu, Q. Wang and Q. Zhao, Phys. Lett. B **757** (2016) 231 [arXiv:1507.05359 [hep-ph]].
64. M. Mikhasenko, arXiv:1507.06552 [hep-ph].
65. U. G. Meiner and J. A. Oller, Phys. Lett. B **751**, 59 (2015) [arXiv:1507.07478 [hep-ph]].
66. V. Kubarovsky and M. B. Voloshin, Phys. Rev. D **92**, no. 3, 031502 (2015) [arXiv:1508.00888 [hep-ph]].
67. H. X. Chen, W. Chen, X. Liu, T. G. Steele and S. L. Zhu, Phys. Rev. Lett. **115**, no. 17, 172001 (2015) [arXiv:1507.03717 [hep-ph]].
68. J. He, Phys. Lett. B **753**, 547 (2016) [arXiv:1507.05200 [hep-ph]].
69. L. Roca, J. Nieves and E. Oset, Phys. Rev. D **92**, no. 9, 094003 (2015) [arXiv:1507.04249 [hep-ph]].
70. R. Chen, X. Liu, X. Q. Li and S. L. Zhu, Phys. Rev. Lett. **115**, no. 13, 132002 (2015) [arXiv:1507.03704 [hep-ph]].
71. C. W. Xiao and U.-G. Meiner, Phys. Rev. D **92**, no. 11, 114002 (2015) [arXiv:1508.00924 [hep-ph]].
72. L. Maiani, A. D. Polosa and V. Riquer, Phys. Lett. B **749**, 289 (2015) [arXiv:1507.04980 [hep-ph]].
73. R. F. Lebed, Phys. Lett. B **749**, 454 (2015) [arXiv:1507.05867 [hep-ph]].
74. G. N. Li, X. G. He and M. He, JHEP **1512**, 128 (2015) [arXiv:1507.08252 [hep-ph]].
75. A. Mironov and A. Morozov, JETP Lett. **102**, no. 5, 271 (201

[arXiv:1507.04694 [hep-ph]].
76. V. V. Anisovich, M. A. Matveev, J. Nyiri, A. V. Sarantsev and A. N. Semenova, arXiv:1507.07652 [hep-ph].
77. R. Ghosh, A. Bhattacharya and B. Chakrabarti, arXiv:1508.00356 [hep-ph].
78. Z. G. Wang, Eur. Phys. J. C **76**, no. 2, 70 (2016) [arXiv:1508.01468 [hep-ph]].
79. Z. G. Wang and T. Huang, Eur. Phys. J. C **76**, no. 1, 43 (2016) [arXiv:1508.04189 [hep-ph]].
80. L. Maiani, A. D. Polosa and V. Riquer, Phys. Lett. B **750**, 37 (2015) [arXiv:1508.04459 [hep-ph]].